Effect of transducer mismatch on the performance of spherical microphone arrays

Dan Rao[12]

[1] Acoustic Lab., Physics Dept., South China University of Technology, Guangzhou, China,

[2] State Key Laboratory of Subtropical Building Science, South China University of Technology,Guangzhou, China

ABSTRACT

Spherical microphone arrays(SMAs) were widely used in sound field recording, beamforming,etc. for its advantage of high geometrical symmetry. Many factors could affect the performance of SMAs, including transducer errors. In this paper, effect of transducer mismatch in amplitude and phase on the performance of SMAs was studied through simulation calculation. A SMAs with 64 nearly uniformly distributed transducers was used in the simulation. Beam patterns with and without transducer mismatch errors were calculated, and then the differences between those patterns were compared using beam pattern correlation coefficients as the metric. The simulation and anlyasis results show that under the condition that the spherical harmonics expansion order is not larger than ka(the product of wave number and array radius), the correlation coefficient is not less than 0.97 when the max random transducer amplitude error is less than 3dB or the maximum random transducer phase error is less than 10 degree. This result indicates that the performance of SMAs has a good tolerance to transducer mismatch errors when spherical harmonics truncation order is not larger than *ka*. While ka less than truncation order, great errors occur due to low-frequency boost nature of SMAs signal processing.

Keywords: Spherical microphone arrays, mismatch, Beamforming, I-INCE Classification of Subjects Number(s): 74.7

1. INTRODUCTION

Spherical microphone arrays (SMAs) are useful for many applications, such as sound field recording, beamforming and sound source localization. Meyer(1) studied SMAs for beamforming. Duraiswami et.al.(2) utilized SMAs to the sound field recording and binaural synthesis. Nilsen et.al(3). proposed spherical harmonics-based ESPRIT localization method using SMAs. Due to the high geometrical symmetry, SMAs have the advantage of unchanged beam pattern for different steering directions. Two types of SMAs are used in general, the open-sphere SMAs and the rigid-sphere SMAs. Because of null solutions in some frequencies, the open-sphere SMAs show more numerical instability than the rigid-sphere SMAs, so the rigid-sphere SMAs are more popular in the practice. Only the rigid-sphere SMAs will be discussed in the following.

Many errors can affect the performance of SMAs, including transducer position errors, measurement noise and transducer mismatch. Rafealy(4) comprehensively studied the effect of position errors, spatial aliasing, measurement noise on the performance of SMAs, in which the array output gain in steering direction was taken as performance metric. The study of the effect of transducer mismatch errors was seldom. In this paper, using beam pattern correlation coefficient as metric, the effects of the transducer mismatch in amplitude and phase on SMAs performance are examined.

[1] phdrao@scut.edu.cn

2. PRINCIPLE

2.1 Beamforming in SMAs

Supposing a unit amplitude plane wave arrives from (θ_s, φ_s) , in the spherical coordinate system, the pressure on a rigid sphere can be written as

$$p(k,a,\theta,\varphi \mid \theta_s,\varphi_s) = \sum_{l=0}^{\infty}\sum_{m=-l}^{l} Y_{lm}^{*}(\theta_s,\varphi_s) b_l(ka) Y_{lm}(\theta,\varphi) \tag{1}$$

Where (a,θ,φ) denotes position on the sphere, a is the radius of the sphere, θ is elevation angle ranged from 0^o to 180^o, φ is azimuth angle ranged from 0^o to 360^o , k is wave number, Y_{lm} are spherical harmonics, which are defined by

$$Y_{lm}(\theta,\varphi) = \sqrt{\frac{(2l+1)(l-m)!}{4\pi(l+m)!}} P_{lm}(\cos\theta) e^{jm\varphi} \tag{2}$$

Where l=0,1,.., m=-l,-l+1…,0,1,..l.

In Eq.(1), $b_l(ka)$ is given by

$$b_l(ka) = 4\pi j^l \left[\frac{j_l(ka)h_l^{'}(ka) - j_l^{'}(ka)h_l(ka)}{h_l^{'}(ka)}\right] \tag{3}$$

Where $j_l(ka)$ and $h_l(ka)$are spherical Bessel and Hankel functions, respectively, j'(ka),h'(ka) are their derivaties.

For SMAs, because microphone transducers arranged on the sphere surface is finite, measuring soud pressure using SMAs is equivalent to sampling pressures on the sphere surface. Multiplying pressures sampled by microphones on the sphere with weights $w^*(\theta_i,\varphi_i)$ and summing them up with weights α_i , it gives the array output

$$A(k,\theta_s,\varphi_s) = \sum_{i=1}^{M} \alpha_i p(k,a,\theta_i,\varphi_i \mid \theta_s,\varphi_s) w^*(\theta_i,\varphi_i) = \sum_{l=0}^{L}\sum_{m=-l}^{l} p_{lm} w_{lm}^{*} \tag{4}$$

Where the weights α_i depend on the sampling scheme, L is the truncation order of spherical harmonics, p_{lm} are the spherical harmonics decomposition of pressure p, M is the microphone number. When the weights w_{lm} are taken as $w_{lm}^{*} = Y_{lm}(\theta_0,\varphi_0)/b_l(ka)$, the array output A in Eq.(4) is regarded as the beam pattern with the steering direction (θ_0,φ_0)

$$\begin{aligned} A(k,\theta_s,\varphi_s \mid \theta_0,\varphi_0) &= \sum_{l=0}^{L}\sum_{m=-l}^{l} p_{lm} Y_{lm}(\theta_0,\varphi_0)/b_l(ka) \\ &= \sum_{i=1}^{M}\sum_{l=0}^{L}\sum_{m=-l}^{l} \alpha_i p(k,a,\theta_i,\varphi_i \mid \theta_s,\varphi_s) Y_{lm}^{*}(\theta_i,\varphi_i) Y_{lm}(\theta_0,\varphi_0)/b_l(ka) \end{aligned} \tag{5}$$

Beam pattern A represents the arrays response for plane wave from different incidence directions while steering at direction (θ_0,φ_0).

Substituting Eq.(1) in Eq.(5), the beam pattern without transducer errors is achieved.

$$A(k,\theta_s,\varphi_s \mid \theta_0,\varphi_0) = \sum_{l=0}^{L}\sum_{m=-l}^{l} Y_{lm}^{*}(\theta_s,\varphi_s) Y_{lm}(\theta_0,\varphi_0) \tag{6}$$

2.2 Effect of Transducer Mismatch

In Eq.(6), the transducers are assumed identical. When the transducer mismatch is considered, Eq.(6) will be revised. Transducer mismatch can be considered as uniformly-distributed random errors in transducer gain and phase. Taking the mismatch error into account, the microphone output become

$$p_i = p_i^o (1+\Delta g_i)\exp(j\Delta\phi_i) \tag{7}$$

Where Δg and $\Delta\Phi$ are amplitude and phase mismatch errors represented by uniformly -distributed random noise.

Substituting Eq.(1) and (7) in Eq.(5) yields the beam pattern with transducer mismatch

$$A(k,\theta_s,\varphi_s \mid \theta_0,\varphi_0) =$$

$$\sum_{i=1}^{M}\sum_{l=0}^{L}\sum_{m=-l}^{l}\alpha_i(1+\Delta g_i)\exp(j\Delta\phi_i)(\sum_{l'=0}^{L'}\sum_{m'=-l'}^{l'}Y_{lm}^{*}(\theta_s,\varphi_s)b_{l'}(ka)Y_{lm}^{*}(\theta_i,\varphi_i))Y_{lm}(\theta_i,\varphi_i)Y_{lm}(\theta_0,\varphi_0)/b_l(ka)$$

$$=\sum_{l=0}^{L}\sum_{m=-l}^{l}\sum_{l'=0}^{L'}\sum_{m'=-l'}^{l'}b_{l'}(ka)/b_l(ka)Y_{lm}^{*}(\theta_s,\varphi_s)Y_{lm}(\theta_0,\varphi_0)e_{ll'mm'} \quad (8)$$

Where $e_{ll'mm'}$ represents the effect of mismatch

$$e_{l'lmm'}=\sum_{i=1}^{M}\alpha_i(1+\Delta g_i)\exp(j\Delta\phi_i)Y_{l'm'}^{*}(\theta_i,\varphi_i)Y_{lm}(\theta_i,\varphi_i) \quad (9)$$

Many studies used the main gain error of A for plane wave from steering direction, i.e. $(\theta_s,\varphi_s)=(\theta_0,\varphi_0)$, as the error metric. However, this metric could not evaluate the beam pattern entirely. Here, a new metric called beam pattern correlation coefficient (BPCC) is proposed, that is

$$a_{cc}=\sum_{i=1}^{N}|A_o(\theta_i,\varphi_i)*A^{*}(\theta_i,\varphi_i)|/\sum_{i=1}^{L}|A_o(\theta_i,\varphi_i)||A(\theta_i,\varphi_i)| \quad (10)$$

Where N is sampling number in beam pattern, A is the actual beam with errors, A^o is the original beam.

BPCC evaluates the similarity between the beam pattern influenced by mismatch error and the original one. For most situations, keeping the shape of beam pattern is more important in practice. The value of BPCC is from 0 to 1, larger BPCC means more similar between these two patterns.

3. Simulations

3.1 Simulation conditions

A SMAs with 64 transducers nearly uniformly arranged on a rigid sphere surface was used in the simulation. The arrangement scheme is shown in Fig.1, which was proposed by Fliege(5).

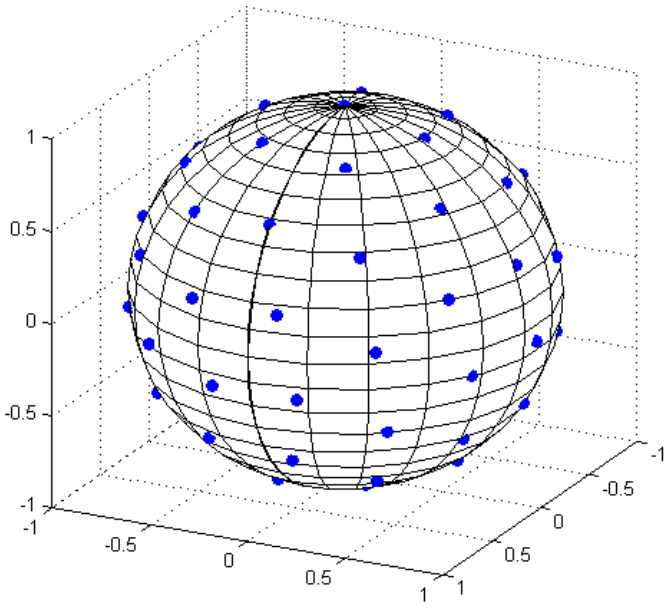

Figure 1 – 64 transducers sampling scheme on a sphere surface.

According to the transducers number, truncation number L=6 was used. When frequencies ka are higher than L, the aliasing error occurs. In order to avoid these errors, only frequencies $ka \le L$ are considered in the following simulation.

As to mismatch errors, maximum amplitude error $|\Delta g|_{max}$ =3dB, 1dB and maximum phase error $|\Delta\Phi|_{max}=10^{o},5^{o}$ are adopted in simulations. BPCC will be calculated as an average over 50 realizations of random errors.

Preliminary simulation found that there was no significant effect of steering direction on error

results, so only one direction((90°,0°)) is calculated in this paper.

3.2 Simulation results

3.2.1 Cases for *ka*=*L*=6

Fig.2 shows magnitudes curve of actual beam pattern A and the original beam pattern A^o in the horizontal plane (θ=90°) under polar coordinates for amplitude mismatch. It can be seen that, the maximum magnitude occurs at (90°,0°) coincident with the steering direction as expected. For the case of $|\Delta g|_{max}$=1dB, two curves are almost coincident, and the BPCC is 0.99. For the case of $|\Delta g|_{max}$=3dB, only slight differences are observed, and the BPCC equals 0.97. These results show, when ka=L the shape of beam pattern keeps very well even if the transducers have relatively large mismatch error.

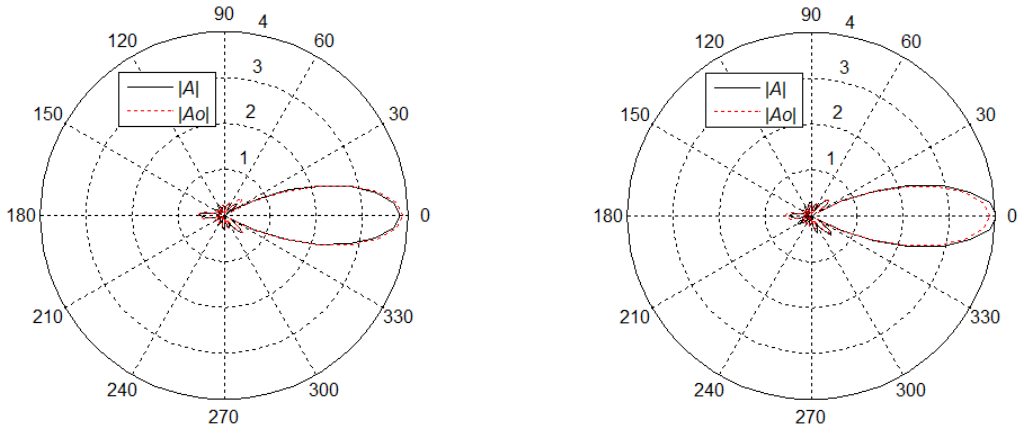

(a) $|\Delta g|_{max}$=1dB,BPCC=0.99 (b) $|\Delta g|_{max}$=3dB,BPCC=0.97

Figure 2 – Beam pattern for amplitude mismatch in the horizontal plane (θ=90°), ka=L=6; red dot line for $|A_o|$, dark solid line for $|A|$

For phase mismatch, magnitude curve is shown in fig.3. Similar to amplitude mismatch cases, 5° error, even 10 ° error only introduces slight impact on the beam pattern.

These results show that the signal processing of SMAs has a good tolerance to transducer mismatch errors.

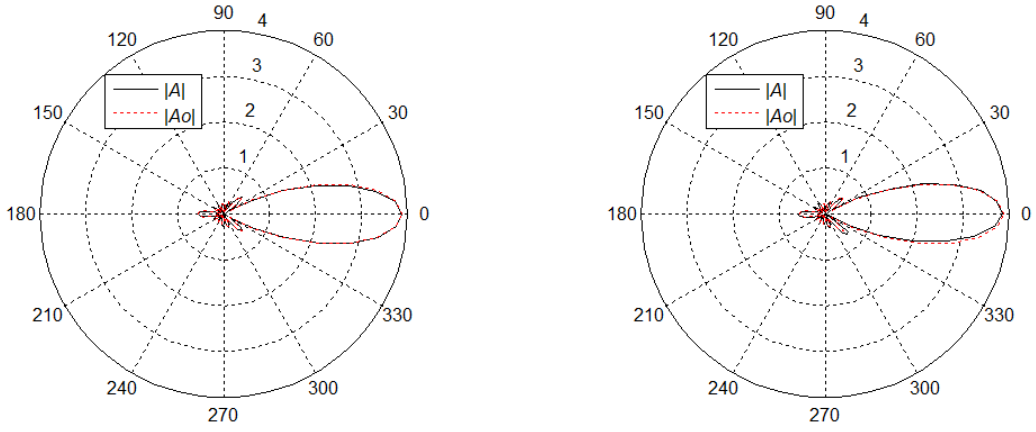

(a) $|\Delta\Phi|_{max}$=5°,BPCC=0.99 (b) $|\Delta\Phi|_{max}$ =10°,BPCC=0.99

Figure 3 – Beam pattern for phase mismatch in the horizontal plane (θ=90°), ka=L=6; red dot line for $|A_o|$, dark solid line for $|A|$

3.2.2 Cases for *ka*<*L*=6

Table.1 shows BPCCs for amplitude mismatch. It can be observed, BPCC decreases with the frequency *ka* decreases. Especially, when *ka*<*L-2*, BPCC dramatically decreases, which indicates the shape of beam pattern is destroyed.

Table 1 – BPCCs for amplitude mismatch

	ka=6	*ka*=5	*ka*=4	*ka*=3	*ka*=2	*ka*=1
$\|\Delta g\|_{max}$=1dB	0.99	0.99	0.97	0.71	0.21	0.11
$\|\Delta g\|_{max}$=3dB	0.97	0.95	0.80	0.33	0.13	0.09

Fig.4 gives beam pattern curve of $|A|$ and $|A_o|$ for $|\Delta g|_{max}$=1dB and *ka*=3,2 respectively. It is shown that, there are very large differences between $|A|$ and $|A^o|$. For the case of *ka*=2, the shape of A could not be identified as originating from A_o. In fact, the term $1/b_l(ka)$ in Eq.(8) will boost when *ka*<*l*. In this way, the effect of mismatch $e_{ll'mm'}$ will be enlarged as *ka* decreases.

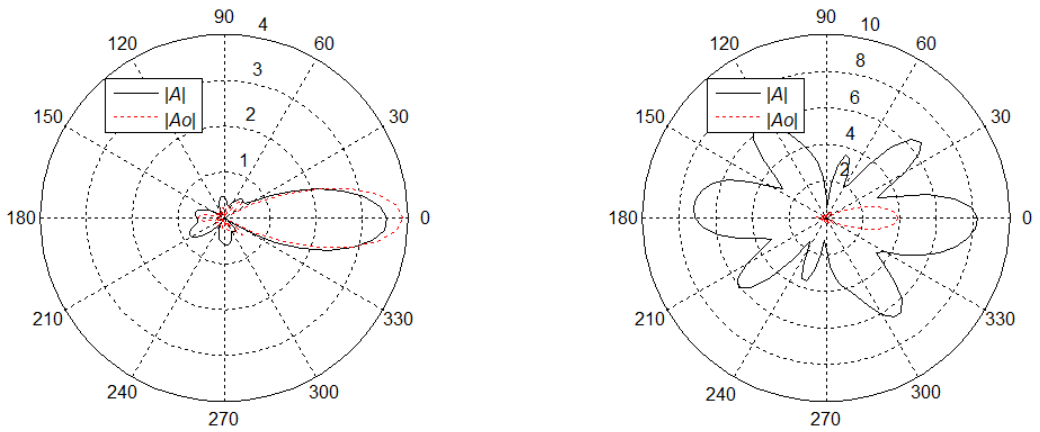

(a) *ka*=3,BPCC=0.71 (b) *ka*=2,BPCC=0.21

Figure 5 – Beam pattern for amplitude mismatch in the horizontal plane (θ=90°), $|\Delta\Phi|_{max}$=5°; red dot line for $|A_o|$, dark solid line for $|A|$

Table.2 shows BPCCs for phase mismatch. Similar behavior for the case of amplitude mismatch is observed. The beam pattern curve for phase mismatch is shown in Fig.5.

Table 2 – BPCC for amplitude mismatch

	ka=6	*ka*=5	*ka*=4	*ka*=3	*ka*=2	*ka*=1
$\|\Delta\Phi\|_{max}$=5°	0.99	0.99	0.98	0.80	0.28	0.14
$\|\Delta\Phi\|_{max}$=10°	0.99	0.99	0.95	0.59	0.18	0.12

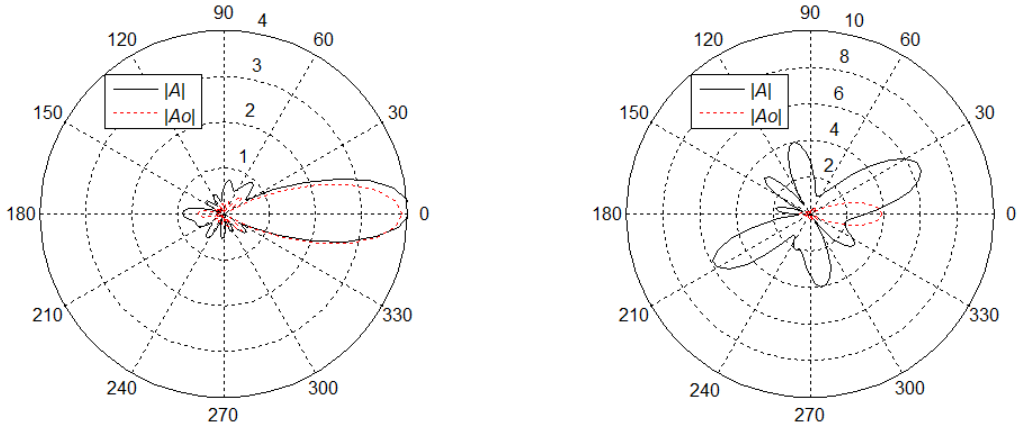

(a) ka=3,BPCC=0.80 (b) ka=2,BPCC=0.28

Figure 5 – Beam pattern for phase mismatch in the horizontal plane (θ=90°), $|\Delta\Phi|_{max}$=5°; red dot line for $|A_o|$, dark solid line for $|A|$

4. CONCLUSIONS

This paper analyzed the effect of transducer mismatch through simulation by using beam pattern correlation coefficient (BPCC) as evaluation metric. When ka=L, relative large mismatch errors, such as 3dB in amplitude error or 10° in phase error, only introduce small error in beam pattern, in which BPCC is larger than 0.97. This result indicates SMAs has a good tolerance to transducer mismatch errors when spherical harmonics truncation order L is not larger than ka. However, when ka is less than L, larger errors occur which is due to the fact $1/b_l(ka)$ will enlarge the mismatch error. So, carefully choosing the truncation order L under certain ka is needed in beamforming processing.

ACKNOWLEDGEMENTS

This work is supported by the State Key Lab of Subtropical Building Science, South China University of Technology, grant no. 2014KB23.

REFERENCES

1. Meyer J, Elko G, Ieee. A highly scalable spherical microphone array based on an orthonormal decomposition of the soundfield. 2002 Ieee International Conference on Acoustics, Speech, and Signal Processing, Vols I-Iv, Proceedings; New York: Ieee; 2002. p. 1781-4.
2. Duraiswami R, Zotkin D, Li Z, Grassi E, Gumerov N, Davis L, editors. High order spatial audio capture and its binaural head-tracked playback over headphones with HRTF cues. AES 119th Conv; 2005; New York, NY.
3. Nilsen C-IC, Hafizovic I, Holm S, editors. Robust 3D sound source localization using spherical microphone arrays 2013; Rome, Italy: Audio Engineering Society.
4. Rafaely B. Analysis and design of spherical microphone arrays. IEEE Transactions on Speech and Audio Processing 2005;13(1):135-43.
5. Fliege J, Maier U. The distribution of points on the sphere and corresponding cubature formulae. Ima Journal of Numerical Analysis 1999 Apr;19(2):317-34.